Optics & Laser Technology 135 (2021) 106723

Contents lists available at ScienceDirect

Optics and Laser Technology

journal homepage: www.elsevier.com/locate/optlastec

Full length article

Intensity-modulated refractometer based on mode-mismatch in surface waveguides inscribed by femtosecond laser direct writing☆

Vítor A. Amorim [a,b,*], Duarte Viveiros [a,b], João M. Maia [a,b], P.V.S. Marques [a,b]

[a] CAP - Centre for Applied Photonics, INESC TEC, Porto 4150-179, Portugal
[b] Department of Physics and Astronomy, University of Porto, Porto 4169-007, Portugal

ARTICLE INFO

Keywords:
Femtosecond laser direct writing
Integrated optical waveguides
Intensity-modulated refractive index sensor
Surface waveguides
Wet-etching

ABSTRACT

Optical waveguides were fabricated at the surface of Eagle2000 glass substrates, using femtosecond laser direct writing and wet etching, and their potential as intensity-modulated refractometers was assessed. Through the analysis of their broadband spectral response to different refractive index oils, we observed that mode mismatch is present when the guided mode reaches the surface of the substrate and interacts with the external medium, thus enabling the use of such optical waveguides in refractive index sensing. Refractive indices equal to or greater than that of the substrate also induced a coupling mechanism that was shown not to be suitable in these devices. The device's wavelength of operation was found to be tunable by controlling the distance between the surface and the center of the optical waveguide. However, the sensitivity was seen to diminish by increasing the latter, being nonexistent for distances greater than 5.5 μm. In this study, the maximum sensitivity values were found for a surface to core center distance between 1 and 2 μm, in the biological range, and 2.5 to 3 μm, for a refractive index nearing that of the substrate. Accordingly, maximum sensitivities of ≈25 dB/RIU and ≈1200 dB/RIU were found between $1.300 < n_D^{25^\circ C} < 1.400$ and $1.490 < n_D^{25^\circ C} < 1.500$, respectively.

1. Introduction

In the last decades, the development of optical sensors using optical fibers has accelerated rapidly. Among several factors, the extremely low losses achieved [1] and its remote sensing capabilities [2] make the optical fibers an excellent platform for the creation of such applications. From the various parameters that can be monitored with an optical fiber, the refractive index stands out as one of the most versatile properties, as it can be explored for chemical and biological sensing [3]. One way of achieving this is by exposing the evanescent field of the guided mode to the external medium. In that sense, the removal of part of the cladding by either polishing or etching [4,5], tapering [6], bending [7], or long period gratings [8] is commonly employed.

Nowadays, we are observing a push for integration. As such, techniques like femtosecond laser direct writing are being utilized to develop optical platforms in optical fibers [9] and bulk substrates [10]. Despite it being a serial process and, thus, a low throughput technique, some materials support very high scan velocities [11,12], severely reducing the fabrication times. This, together with its three-dimensional capabilities and prototyping flexibility, turn it into a versatile tool. In the case of bulk substrates, the evanescent field of the guided mode can be exposed to an external medium by either the inscription of waveguides nearing the sidewall of a microfluidic channel [13,14] or the surface of the substrate [15–20].

Intensity modulation is an attractive interrogation scheme, as it is associated with simplicity and low cost. This comes mostly from the replacement of complex light emitting sources and optical spectrum analyzers by light-emitting diodes and photodetectors. As such, it is not surprising that the application of intensity modulation has already been reported in the development of refractive index sensors, and more specifically in those where the evanescent field of the guided mode is exposed so that the transmission is seen to depend on the external

☆ This work was supported by Fundação para a Ciência e a Tecnologia through grant no. SFRH/BD/128795/2017 and by Project "On Chip Whispering Gallery Mode Optical Microcavities For Emerging Microcontaminant Determination In Waters" - SAFE WATER, which is supported and co-funded by the European Commission, Directorate-General Communications Networks, Content and Technology (DG CONNECT) under the ERA-NET Cofund scheme - Horizon 2020 "Horizon 2020 – the Framework Programme for Research and Innovation (2014-2020)".

* Corresponding author.
E-mail addresses: vitor.a.amorim@inesctec.pt (V.A. Amorim), carlos.d.viveiros@inesctec.pt (D. Viveiros), joao.m.maia@inesctec.pt (J.M. Maia), psmarque@fc.up.pt (P.V.S. Marques).

https://doi.org/10.1016/j.optlastec.2020.106723
Received 28 June 2020; Received in revised form 24 October 2020; Accepted 27 October 2020
Available online 12 November 2020

medium's refractive index. Different methods of achieving this have been tested. In optical fibers, side-polishing has been used to obtain D-shaped fibers whose core nears the boundary between the cladding and the external medium [21–24]. The use of tapered optical fibers has also been tested, with PDMS being used to embed the taper with microfluidic channels [25]. Also, the removal of the optical fiber's cladding has shown to be effective in the exposure of the guided mode to external media [26]. In devices developed by femtosecond laser writing, the production of optical waveguides near or at the surface of PMMA, Gorilla glass and silver-containing zinc phosphate glass substrates has also proved the capability of such sensing platforms [12,27,28]. Still, these studies were conducted with well confined guided modes, limiting the amount of evanescent field interacting with the external medium, and, therefore, the sensitivity of the devices.

In this work, we report the refractive index sensing capabilities of optical waveguides produced at the surface of Eagle2000 substrates, using femtosecond laser direct writing and wet etching, and whose guided mode nears the cut-off. To understand the underlying mechanisms responsible for the sensitivity, the impact of different refractive index oils in the broadband spectral response of the waveguides was studied—from 500 to 1700 nm—below and above the substrate's refractive index. Finally, an analysis of the dependence of the device's sensitivity to refractive index, wavelength of operation, and waveguide depth was performed.

2. Experimental procedure

A fiber amplified femtosecond laser (Satsuma HP, from Amplitude Systèmes)—operating at 515 nm with a pulse duration of ≈ 250 fs and a repetition rate of 1 MHz—was employed in the inscription of optical waveguides in alkali-free boro-aluminosilicate glass (Eagle2000). Together with the femtosecond laser was a Workshop of Photonics workstation equipped with Aerotech direct-drive stages (ANT130XY-110 PLUS and ANT130V-5 PLUS) and a 0.42 numerical aperture plan apochromat objective (Mitutoyo M Plan Apo NIR 50x) that was used to produce the structures at a minimum depth of ≈ 25 μm. The laser beam was set orthogonal to the scan direction while keeping its linear polarization parallel to the writing direction. The scan direction was maintained in order to avoid the Quill effect [29]. Pulse energy and scan velocity were fixed at 125 nJ and 6 cm/s, respectively. This choice of parameters is substantiated in two previous works of ours [11,20], as they were shown to yield low-scattering waveguides whose propagation loss is mostly limited by material absorption. Furthermore, single-mode operation starts at roughly 800 nm, with longer wavelengths nearing its cut-off. As such, the guided mode is larger, increasing the effect that the external medium has on the performance of the sensing devices. The optical waveguides were then translated to the surface through wet etching, using a solution composed of HF 1%/HCl 37% 10/2 (V/V) as to avoid surface roughness [20]. Before characterization, the side facets of the substrate were polished to remove any defects induced by the laser as it crossed the air/glass boundary and the presence of etching selectivity from the etching process. To determine the waveguides' spectral response, a broadband source was coupled to a single-mode fiber (SMF-28), which in turn was butt-coupled to the entrance facet of the inscribed optical waveguides. The transmitted signal was then collected by a second butt-coupled optical fiber at the exit facet and guided to an optical spectrum analyzer (ANDO AQ-6315B), where it was inspected from 500 to 1700 nm with a 10 nm resolution. To remove the source's spectral characteristics from the collected signal, a normalization was made to all transmission spectra. The alignment of the butt-coupling optical fibers with the produced devices was achieved in an Elliot Martock MDE881 stage with piezo controls (Dali E-2100). Fresnel reflections at both input/output fibers/facets were minimized with the use of index matching fluid (Cargille series: AA $n_D^{25°C} = 1.4580 \pm 0.0002$).

3. Experimental results and discussion

In this study, several 24 mm long optical waveguides were fabricated in Eagle2000 while varying the surface to core center distance in steps of 0.5 μm. Of the 24 mm, 8 mm were inscribed closer to the surface as to both enable and limit the distance in which the guided mode and the external medium can interact. For this purpose, 3.5 mm long sine-generated vertical S-bends—with a minimum curvature radius of 125 mm—were used to raise the central portion of the waveguide 20 μm closer to the surface, as depicted in Fig. 1. Such feature also ensures the protection of the waveguide's end facets from the fragile edges of the glass substrate. The cross-section of the waveguides' sensing region is depicted in Fig. 2 for a surface to core center distance between 0 and 7 μm. Here, it is also possible to observe that, for smaller separations, the partial removal of the top of the inscribed optical waveguides is accompanied by residual etching anisotropy between exposed and non-exposed volumes. This effect is purely morphological. In order to study the capability of these waveguides as refractometers, air and multiple Cargille refractive index oils (1.300 to 1.640, $n_D^{25°C}$) were placed on top of the substrate—covering the entirety of the interaction region—and the response of the waveguides characterized.

Fig. 3 (a) depicts the insertion loss, as a function of wavelength, of an optical waveguide with a surface to core center distance of 3 μm for different Cargille refractive index oils between 1.000 and 1.500 ($n_D^{25°C}$). As can be seen, the insertion loss increases monotonically for wavelengths greater than 1200 nm, with the slope decreasing for oils with a larger refractive index. By normalizing the different insertion loss spectra to the spectrum retrieved in air and then plotting it for a wavelength of 1512 nm, the effect of larger refractive indices becomes clear; as can be seen in Fig. 3 (c), the transmitted power increases monotonically with the oil's refractive index (n_{oil}), with the amount of transmitted light increasing dramatically as n_{oil} approaches the refractive index of the glass substrate (n_{glass}, n_D=1.5068). Such behavior, although not as distinct, has already been observed in other works [12,23,25,28]. In [20], we demonstrated the influence that the air-glass refractive index contrast at the surface has on the spectral characteristics of waveguides at different depths. More specifically, we found that the insertion loss at longer wavelengths increases as the waveguides approach the surface. Such behavior was attributed to coupling loss due to the deformation of the propagating mode as it approaches the refractive index contrast at the surface. Thus, the behavior observed in Fig. 3 (a, c) can be explained as follows. Coupling loss—arising from mode deformation—is present due to the air-glass interface, with its effect becoming more intense for longer wavelengths due to an increasingly larger mode field diameter. Its influence in the overall guiding characteristics of the waveguide is, however, reduced as the refractive index contrast decreases for higher values of n_{oil}. When n_{oil} matches n_{glass}, the propagating mode is not perturbed, and the spectral response of the waveguide resembles that of a buried waveguide. This reasoning is corroborated by simulations of the mode profile (see Fig. 4) and is also in accordance with the work developed in [28].

Moreover, the $n_{oil} > n_{glass}$ region has also been targeted in other studies [12,23,25,27,28]. As such, the response of a waveguide—with a surface to core center distance of 8 μm—to n_{oil} between $1.000 < n_D^{25°C} < 1.640$ is depicted in Fig. 3(d). In this case, the behavior still matches that at Fig. 3(c) for $n_{oil} \leq n_{glass}$, although with a much smaller peak due to the

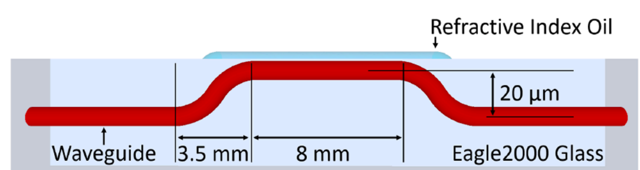

Fig. 1. Schematic of the devices fabricated and studied in this work.

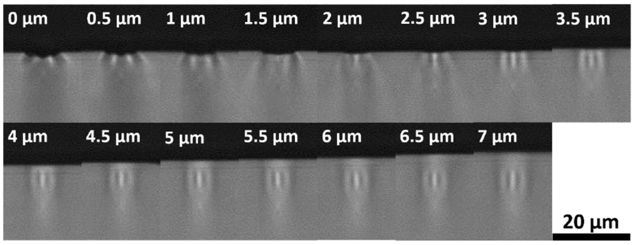

Fig. 2. Transmission mode optical microscope images of the cross-section of modification tracks produced in Eagle2000 and brought to the surface by wet etching. Laser inscription was made from the top to the bottom.

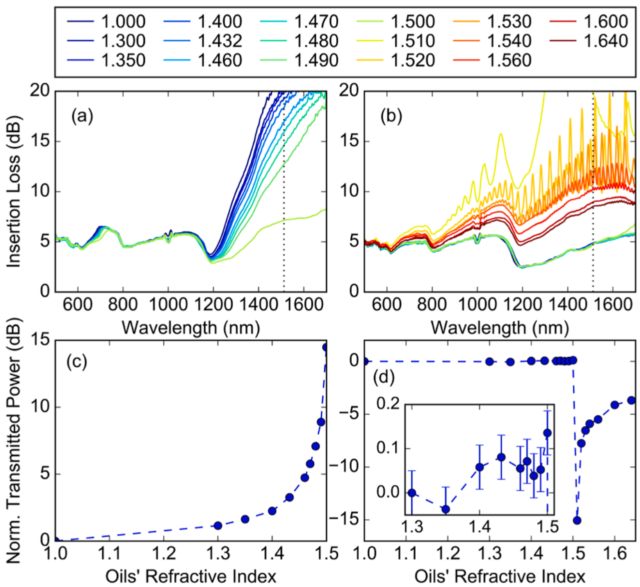

Fig. 3. Insertion loss, as a function of wavelength, and normalized transmitted power of two optical waveguides exposed to different Cargille refractive index oils at a surface to core center distance of 3 µm (a, c) and 8 µm (b, d). The normalized transmitted power was calculated at 1512 nm—indicated in (a) and (b) by the vertical dotted lines—through the subtraction of all insertion loss spectra with that of a waveguide exposed to air.

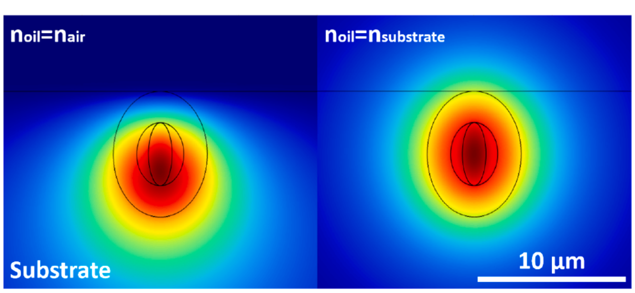

Fig. 4. Simulated mode profile (electric field norm) for different external media, namely air and an external medium with a refractive index equal to that of the substrate. The simulation was made at 1550 nm, using COMSOL Multiphysics. The refractive index of the substrate was set to 1.496, while the refractive index variation, in relation to the substrate, of the waveguide's inner, intermediate, and outer regions were set to 0.007, −0.001, and 0.003, respectively. These values took into consideration the refractive index measurements performed by Arriola et al. [30]. The dimensions used in the structure tried to represent as close as possible the waveguide's cross-section.

larger surface to core center separation and, therefore, a more noticeable uncertainty arising from the alignment of the input and output fibers (see inset). However, when n_{oil} matches the effective refractive index of the guided mode (n_{eff}), the amount of light transmitted decreases sharply, increasing again for $n_{oil} > n_{eff}$ despite never reaching the levels found when $n_{oil} \leq n_{glass}$. It should also be noted that the decrease in normalized transmitted power is much more pronounced for a smaller surface to core center distance, getting below the noise level of the detector in some cases and the reason why we plotted the data for a separation of 8 µm. It is also easy to see how misleading Fig. 3(d) is. Looking at Fig. 3(b), one can observe that the spectral response for $n_{oil} > n_{glass}$ presents several dips in transmission whose strength and periodicity increases with wavelength, both decreasing for greater n_{oil}. This means that a small shift in the monitored wavelength will create a very dissimilar output, possibly explaining the difficulties encountered by Khalil et al. in fitting their model to the experimental data in this region [28]. Upon closer inspection, the nature of these spectra resembles that of a directional coupler. Indeed, the refractive index oil forms a film above the substrate that can act as a planar waveguide. Energy transfer may occur between such planar waveguide and the (three-dimensional) laser-written waveguide which is found in close proximity to the surface. As such, when $n_{oil} \approx n_{eff}$, the phase matching is optimal and the energy transfer between both waveguides should be complete. However, the confinement in planar waveguides is one dimensional, meaning that the loss of light as it propagates is inevitable, revealing why, despite the dips, the amount of light never reaches that of $n_{oil} \leq n_{glass}$. When $n_{oil} > n_{eff}$, the phase-matching condition is not satisfied and the coupling efficiency decreases rapidly, limiting the amount of light that is transferred to the oil film and, subsequently, the dip size, with the guided mode behaving at this point as a leaky mode. Furthermore, the response should depend on the thickness of the oil's film, a feature that is not desirable in a refractometer. Therefore, the $n_{oil} > n_{glass}$ region should only be analyzed when the external medium is considered semi-infinite, a condition that is not met in this work and the reason why this study was restricted to the $n_{oil} \leq n_{glass}$ region.

Fig. 5(a) displays the normalized transmitted power as a function of wavelength and refractive index for a surface to core center distance between 0 and 7 µm. Regions with excessive noise due to high coupling losses were removed and are represented as white in the contour plots. Looking at the data, one can observe that the behavior depicted in Fig. 3(c) encompasses all surface to core center distances tested, with the normalized transmitted power reaching a variation of up to 20 dB. Furthermore, this behavior is seen to depend on the wavelength and surface to core center distance. For a separation distance between 2.5 and 5 µm, one can notice that the change in normalized transmitted power appears to be restricted to a limited wavelength interval, suggesting that this behavior is transversal to the other separation distances tested. Unfortunately, this hypothesis could not be confirmed due to the insufficient signal to noise ratio, in the 0 to 2 µm range, and the limited wavelength window, for a separation distance greater than 5 µm. Nevertheless, if confirmed, the nature of this behavior should be twofold. First, the increase in mode field diameter with wavelength, which increases its interaction with the external medium and, therefore, explains the increase in normalized transmitted power found at the shorter side of the wavelength interval. And second, the geometry of the waveguide, since in [20] we found that light lost at the first S-bend is recoupled at the last, creating an upper limit in the insertion loss at longer wavelengths that suppresses the change in transmitted power for lower n_{oil}. The location of this limited wavelength interval also depends on the surface to core center distance. More specifically, the wavelength interval is observed to redshift for a larger separation distance. This has to do with the evolution of the cut-off verified at longer wavelengths, as the cut-off was seen to increase in wavelength with the increase in surface to core center distance [20]. Additionally, Fig. 5(a) also shows that the change in normalized transmitted power decreases as the

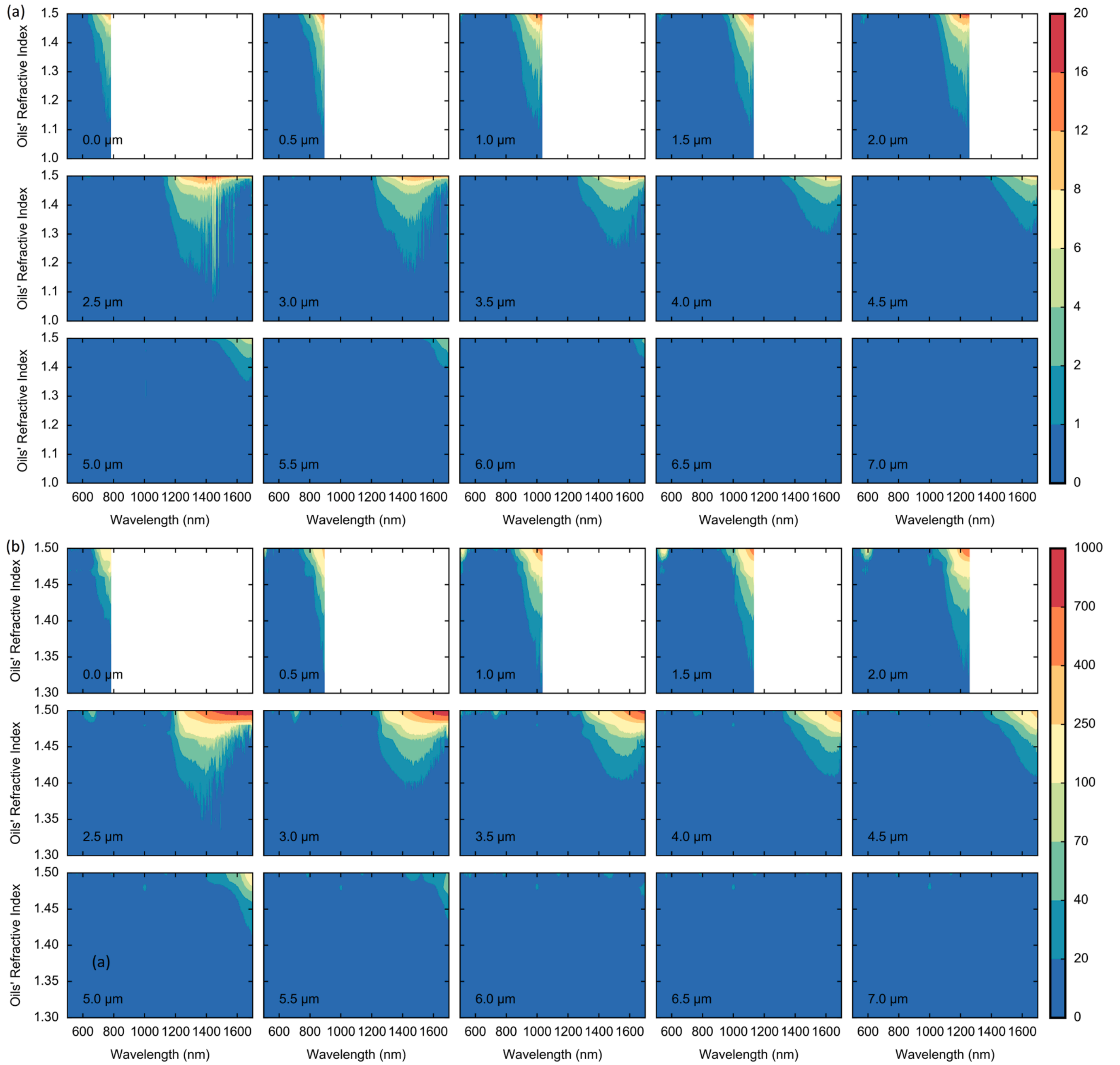

Fig. 5. Normalized transmitted power (dB, a) and sensitivity (dB/RIU, b) of optical waveguides exposed to different Cargille refractive index oils ($n_D^{25^\circ C}$ between 1.300 and 1.500) in a wavelength range between 500 and 1700 nm and for a surface to core center distance between 0 and 7 µm.

surface to core center distance increases. This is due to the declining interaction between the guided mode and the external medium, demonstrating the importance of the capability of tuning the depth at which these waveguides are produced.

Fig. 5(b) presents the sensitivity of the near-surface waveguides to the refractive index of the oil's film as a function of wavelength and refractive index for a surface to core center distance between 0 and 7 µm. To create each of these contour maps, the corresponding plots in Fig. 5 (a) had to be decomposed in all the wavelengths sampled in order to obtain multiple data sets like the one present in Fig. 3(c). Then, the first-order central difference approximation of the derivative of the normalized transmitted power was utilized for every data set, with the first-order forward and backward difference being utilized in the first and last point of each data set, respectively. It is also important to mention that, to facilitate the creation of these contour maps, the sensitivity was calculated without taking dispersion into account, and is, therefore, represented for the sodium D lines (589.3 nm). As expected, the sensitivity maps resemble those of the normalized transmitted power. Sensitivity is seen to increase with n_{oil}, reaching up to ≈1000 dB/RIU for a surface to core center distance between 2.5 and 3 µm. Also, the redshift of the window of interest with the increase of the surface to core center distance meant that, for separations larger than 5.5 µm, the devices developed do not possess sensitivity in the range of parameters tested. This shows that even with a relatively small separation, the guided mode does not interact with the external medium, demonstrating, again, the importance of placing the waveguides at the surface. Additionally, the wavelength at which the sensitivity is maximized depends on the refractive index of the oil film, with a redshift being observed for greater n_{oil}. As discussed previously, this behavior is due to a limitation in the manufactured structures, since a small portion of the light is lost at the first S-bend and then recoupled at the last without interacting with the external medium, suppressing the sensitivity for lower n_{oil}. Ideally, the inexistence of this flaw would enable the sensitivity to increase with wavelength, providing higher sensitivities at both smaller (in the biological range, i.e. $n_D^{25^\circ C} \approx 1.33$) and greater refractive indices (at the n_{glass} limit).

As it stands, the maximum sensitivity values were found for a surface to core center distance between 1 and 2 μm, in the biological range, and 2.5 to 3 μm, for a refractive index nearing n_{glass}. Dispersion corrected sensitivity values between $1.300 < n_D^{25^\circ C} < 1.400$ and $1.490 < n_D^{25^\circ C} < 1.500$ were found to be ≈25 dB/RIU and ≈1200 dB/RIU, respectively. Furthermore, these can still be improved by reducing the amount of light that does not interact with the surface, as discussed above, making the noise level of the optical spectrum analyzer/power meter the limitation of such device. Additionally, the n_{glass} limit can be extended with the use of materials of higher refractive index, with lower refractive index materials enabling better sensitivities in the biological range.

4. Conclusion

In this work, we demonstrated that optical waveguides produced at the surface of Eagle2000 substrates can be used as intensity-modulated refractometers. This was found to be especially true for refractive indices up to that of the glass substrate, where the principle responsible for this effect is based on the mode mismatch that occurs when the guided mode reaches the surface of the substrate and interacts with the external medium. For refractive indices greater than that of the glass substrate, the analysis of the broadband spectra revealed that the intensity modulation is most likely due to the transition of energy between the waveguide and the film produced by the refractive index oil, making the spectral response dependent on the film's thickness and, therefore, causing the device to be unreliable as an intensity-modulated refractometer. Still, the use of a thicker external medium may enable the use of this mechanism in refractive index sensing. Moreover, the device's sensitivity was shown to be localized within a wavelength interval that depends on the surface to core center distance, meaning that the device's wavelength of operation can be tuned accordingly. However, the sensitivity was also seen to decrease for larger surface to core center distances, being nonexistent for distances greater than 5.5 μm. Additionally, the wavelength at which the sensitivity is maximized suffers a redshift as the refractive index increases. This can, in principle, be corrected by implementing less abrupt S-bends. Nevertheless, the maximum sensitivity values were found for a surface to core center distance between 1 and 2 μm, in the biological range, and 2.5 to 3 μm, for a refractive index nearing that of the substrate. Maximum sensitivity values of ≈25 dB/RIU and ≈1200 dB/RIU were found between $1.300 < n_D^{25^\circ C} < 1.400$ and $1.490 < n_D^{25^\circ C} < 1.500$, respectively, demonstrating the potential of poorly confined optical modes in mode-mismatch based intensity-modulated sensing. Unfortunately, the lack of sensitivity at the biological range limits, to some extent, the applicability of these sensors. However, the use of polymeric films whose refractive index falls in the range of greater sensitivity, such as poly(vinyl alcohol), poly(acrylic acid), and poly(ethylene-co-vinyl acetate), can be used to produce, for instance, pH [31], humidity [22], or even putrescine (a potential indicator of food deterioration) [32] sensors.

Declaration of Competing Interest

The authors declare that they have no known competing financial interests or personal relationships that could have appeared to influence the work reported in this paper.

References

[1] T. Miya, Y. Terunuma, T. Hosaka, T. Miyashita, Ultimate low-loss single-mode fibre at 1.55 μm, Electronics Lett. 15 (4) (Feb 1979) 106–108.

[2] M. Fernandez-Vallejo, M. Lopez-Amo, Optical fiber networks for remote fiber optic sensors, Sensors 12 (4) (Mar 2012) 3929–3951.

[3] M. Pospíšilová, G. Kuncová, J. Trögl, Fiber-optic chemical sensors and fiber-optic bio-sensors, Sensors 15 (10) (Oct 2015) 25208–25259.

[4] R. Slavík, J. Homola, J. Cyroký, E. Brynda, Novel spectral fiber optic sensor based on surface plasmon resonance, Sens. Actuat. B 75 (1–3) (Apr 2001) 106–111.

[5] L. Coelho, J.M.M.M. Almeida, J.L. Santos, R.A.S. Ferreira, P.S. André, D. Viegas, Sensing structure based on surface plasmon resonance in chemically etched single mode optical fibres, Plasmonics 10 (2) (Apr 2015) 319–327.

[6] H. Lin, C. Huang, G. Cheng, N. Chen, H. Chui, Tapered optical fiber sensor based on localized surface plasmon resonance, Opt. Exp. 20 (20) (Sep 2012) 21693–21701.

[7] A.S. Arcas, F.S. Dutra, R.C.S.B. Allil, M.M. Werneck, Surface plasmon resonance and bending loss-based u-shaped plastic optical fiber biosensors, Sensors 18 (2) (2018), 648.

[8] H.C.A.S.G. Vasconcelos, J.M.M.M. Almeida, C.M.T. Saraiva, P.A.S. Jorge, L.C. C. Coelho, Mach-Zehnder interferometers based on long period fiber grating coated with titanium dioxide for refractive index sensing, J. Lightwave Technol. 37 (18) (Sep. 2019) 4584–4589.

[9] J.R. Grenier, L.A. Fernandes, P.R. Herman, Femtosecond laser inscription of asymmetric directional couplers for in-fiber optical taps and fiber cladding photonics, Opt. Express 23 (13) (Jun 2015) 16760–16771.

[10] V.A. Amorim, J.M. Maia, D. Alexandre, P.V.S. Marques, Monolithic add-drop multiplexers in fused sílica fabricated by femtosecond laser direct writing, J. Lightwave Technol. 35 (17) (Sep 2017) 3615–3621.

[11] V.A. Amorim, D. Viveiros, J.M. Maia, P.V.S. Marques, Mass producible low-loss broadband optical waveguides in Eagle 2000 by femtosecond laser writing, IEEE Photon. Technol. Lett. 31 (20) (Oct 2019) 1658–1661.

[12] J. Berubé, C. Frayssinous, J. Lapointe, S. Duval, V. Fortin, R. Vallée, Direct inscription of on-surface waveguides in polymers using a mid-ir fiber laser, Opt. Exp. 27 (21/14) (Oct 2019) 31013–31022.

[13] V. Maselli, J.R. Grenier, S. Ho, P.R. Herman, Femtosecond laser written optofluidic sensor: Bragg grating waveguide evanescent probing of microfluidic channel, Opt. Exp. 17 (14) (Jul 2009) 11719–11729.

[14] J.M. Maia, V.A. Amorim, D. Alexandre, P.V.S. Marques, Real-time optical monitoring of etching reaction of microfluidic channel fabricated by femtosecond laser direct writing, J. Lightwave Technol. 35 (11) (Jun 2017) 2291–2298.

[15] J. Lapointe, M. Gagné, M. Li, R. Kashyap, Making smart phones smarter with photonics, Opt. Exp. 22 (13) (Jun 2014) 15473–15483.

[16] E. Zgraggen, O. Scholder, G. Bona, F. Fontana, E. Alberti, A. Crespi, R. Osellame, T. Scharf, I. Shorubalko, Optical properties of waveguide-coupled nanowires for sub-wavelength detection in microspectrometer applications, J. Opt. 17 (2) (2015), 025801.

[17] J. Bérubé, R. Vallée, Femtosecond laser direct inscription of surface skimming waveguides in bulk glass, Opt. Lett. 41 (13) (Jul 2016) 3074–3077.

[18] J. Martínez, A. Ródenas, A. Stake, M. Traveria, M. Aguiló, J. Solis, R. Osellame, T. Tanaka, B. Berton, S. Kimura, N. Rehfeld, F. Díaz, Harsh-environment-resistant OH-vibrations-sensitive mid-infrared water-ice photonic sensor, Adv. Mater. Technol. 2 (8) (2017), 1700085.

[19] H.O. Çirkinoglu, M.M. Bayer, U.S. Gokay, A. Serpenguzel, B. Sotillo, V. Bharadwaj, R. Ramponi, S.M. Eaton, Silicon microsphere whispering gallery modes excited by femtosecond-laser-inscribed glass waveguides, Appl. Opt. 57 (14) (May 2018) 3687–3692.

[20] V.A. Amorim, J.M. Maia, D. Viveiros, P.V.S. Marques, Inscription of surface waveguides in glass by femtosecond laser writing for enhanced evanescent wave overlap, J. Opt. 22 (8) (2020), 085801.

[21] S. Tseng, C. Chen, Side-polished fibers, Appl. Opt. 31 (18) (Jun 1992) 3438–3447.

[22] A. Gastón, F. Pérez, J. Sevilla, Optical fiber relative-humidity sensor with polyvinyl alcohol film, Appl. Opt. 43 (21) (Jul 2004) 4127–4132.

[23] L. Bilro, N. Alberto, J.L. Pinto, R.N. Nogueira, A simple and low-cost cure monitoring system based on a side-polished plastic optical fibre, Meas. Sci. Technol. 21 (11) (2010), 117001.

[24] F. Sequeira, N. Cennamo, A. Rudnitskaya, R. Nogueira, L. Zeni, L. Bilro, D-shaped POF sensors for refractive index sensing-The importance of surface roughness, Sensors 19 (11) (2019), 2476.

[25] P. Polynkin, A. Polynkin, N. Peyghambarian, M. Mansuripur, Evanescent field-based optical fiber sensing device for measuring the refractive index of liquids in microfluidic channels, Opt. Lett. 30 (11) (Jun 2005) 1273–1275.

[26] A. Banerjee, S. Mukherjee, R.K. Verma, B. Jana, T.K. Khan, M. Chakroborty, R. Das, S. Biswas, A. Saxena, V. Singh, R.M. Hallen, R.S. Rajput, P. Tewari, S. Kumar, V. Saxena, A.K. Ghosh, J. John, P. Gupta-Bhaya, Fiber optic sensing of liquid refractive index, Sens. Actuat. B 123 (1) (Apr 2007) 594–605.

[27] J. Lapointe, F. Parent, E.S.L. Filho, S. Loranger, R. Kashyap, Toward the integration of optical sensors in smartphone screens using femtosecond laser writing, Opt. Lett. 40 (23) (Dec 2015) 5654–5657.

[28] A.A. Khalil, P. Lalanne, J. Bérubé, Y. Petit, R. Vallée, L. Canioni, Femtosecond laser writing of near-surface waveguides for refractive-index sensing, Opt. Exp. 27 (22/28) (Oct 2019) 31130–31143.

[29] P.G. Kazansky, W. Yang, E. Bricchi, J. Bovatsek, A. Arai, Y. Shimotsuma, K. Miura, K. Hirao, Quill writing with ultrashort light pulses in transparent materials, Appl. Phys. Lett. 90 (15) (2007), 151120.

[30] A. Arriola, S. Gross, N. Jovanovic, N. Charles, P.G. Tuthill, S.M. Olaizola, A. Fuerbach, M.J. Withford, Low bend loss waveguides enable compact, efficient 3D photonic chips, Opt. Exp. 21 (3) (Feb 2013) 2978–2986.

[31] W.C. Wong, C.C. Chan, P. Hu, J.R. Chan, Y.T. Low, X. Dong, K.C. Leong, Miniature pH optical fiber sensor based on waist-enlarged bitaper and mode excitation, Sens. Actuat. B 191 (Feb 2014) 579–585.

[32] H. Vasconcelos, J.M.M.M. Almeida, C. Saraiva, D. Viveiros, P.A.S. Jorge, L. Coelho, Preliminary assessment on the detection of putrescine using long period fiber

gratings coated with titanium dioxide and poly(ethylene-co-vinyl acetate), Proc. of SPIE 11354 (2020), 113540B.